A Possible Family of B-like Triple Helix Structures: Comparison with the Arnott A-like Triple Helix

Mohammed Ouali,[‡] Richard Letellier,[‡] Frédéric Adnet,[‡] Jean Liquier,[‡] Jian-Sheng Sun,[§] Richard Lavery,[∥] and Eliane Taillandier*,[‡]

Laboratoire CSSB, URA CNRS 1430, UFR Santé Médecine et Biologie Humaine, Université Paris XIII, 74, rue Marcel Cachin, 93012 Bobigny, France, Laboratoire de Biophysique, Museum National d'Histoire Naturelle, INSERM U201, CNRS URA481, 43, rue Cuvier, 75231 Paris Cedex 05, France, and Laboratoire de Biochimie Théorique, Institut de Biologie Physico-Chimique, CNRS URA77, 13, rue Pierre et Marie Curie, 75005 Paris, France

Received August 11, 1992; Revised Manuscript Received November 12, 1992

ABSTRACT: Recent experimental studies of the structure of triple helices show that their conformation in solution differs from the A-like structure derived from diffraction data on triple helix fibers by Arnott and co-workers. Here we show by means of molecular modeling that a family of triple helix structures may exist with similar conformational energies, but with a variety of sugar puckers. The characteristics of these putative triple helices are analyzed for three different base sequences: $(T{\cdot}A{\times}T)_n$, $(C{\cdot}G{\times}C^+)_n$, and alternating $(C{\cdot}G{\times}C^+/T{\cdot}A{\times}T)_n$. In the case of $(C{\cdot}G{\times}C^+)_n$ triple helix, infrared and Raman spectra have been obtained and clearly reveal the existence of both N- and S-type sugars in solution. The molecular mechanics calculations allow us to propose a stereochemically reasonable model for this triple helix, in good agreement with the vibrational spectroscopy results.

Interest in triple-stranded DNA has greatly increased in recent years following the discovery of triple helix formation in vivo (Mirkin et al., 1987) and the implication that DNA triple helices may play an important regulatory role for biological functions (Le Doan et al., 1987; Moser & Dervan, 1987; Wells et al., 1988). Homopyrimidine oligonucleotides can bind to homopurine–homopyrimidine tracts of double-stranded DNA (Mirkin et al., 1987; Le Doan et al., 1987; Lyamichev et al., 1988; Moser & Dervan, 1987; Wells et al., 1988), and this could give rise to important developments in the conception of new DNA binding reagents. Oligonucleotide-directed triple helix formation may also be used for chromosome analysis, gene mapping (Moser & Dervan, 1987; Hélène et al., 1989; Strobel & Dervan, 1990), and the artificial control of gene expression (François et al., 1989; Maher et al., 1989). Potential therapeutic applications such as the suppression of unwanted gene expression in vivo, so-called genetic medication, are also conceivable with such molecules. Nevertheless, it is obvious that the development of such applications requires an accurate knowledge of the conditions of triple helix formation, of their stability, and of their structure.

Pioneering studies of triple helix structures were performed more than 15 years ago by Arnott and co-workers (Arnott & Bond, 1973; Arnott & Selsing, 1974; Arnott et al., 1976). These authors proposed triple helical conformations for $(U{\cdot}A{\times}U)_n$ (Arnott & Bond, 1973) and for $(T{\cdot}A{\times}T)_n$ (Arnott & Selsing, 1974; Arnott et al., 1976) based on fiber diffraction data. In the notation X·Y×Z the "·" represents Watson–Crick pairing between the homopyrimidine strand I and the homopurine strand II, while the "×" represents Hoogsteen pairing between strand II and the homopyrimidine strand III. The Arnott model resembles the duplex structure of A-DNA, and all sugars were assigned to the C3′-endo conformation (N-type) characteristic of this allomorph. In contrast, recent structural investigations by NMR (Rajagopal et al., 1989; Santos et al., 1989; Macaya et al., 1992) and vibrational spectroscopy (Thomas & Peticolas, 1983; Liquier et al., 1991) have gathered evidence that triple helices in fact contain sugars with more than one type of pucker. Notably, Raman spectroscopy has shown that the wavenumbers of lines reflecting the sugar geometries in $(T{\cdot}A{\times}T)_n$ triplexes do not fall in the normal range for the A-genus (N-type) and seem to be indicative of differing forms of the B-genus (S-type). Similarly, Fourier transform infrared spectra (FTIR) of $(T{\cdot}A{\times}T)_n$ (Liquier et al., 1991) have confirmed that, in solution, the sugars belong mainly to the C2′-endo family (S-type).

In the present work, we use molecular mechanics to show that conformations of (Pyr)·(Pur)×(Pyr) triple helices which differ from the A-like Arnott model are both stereochemically and energetically reasonable. We presently study three base sequences: $(T{\cdot}A{\times}T)_n$, $(C{\cdot}G{\times}C^+/T{\cdot}A{\times}T)_n$, and $(C{\cdot}G{\times}C^+)_n$. In the latter case, the model geometries have been compared to the results obtained by vibrational spectroscopy. Raman and FTIR spectra of $(C{\cdot}G{\times}C^+)_n$ show the existence of both N- and S-type sugars within this triple helix and have allowed the sugar conformation of each strand to be determined. The theoretically derived conformation is found to be in good agreement with these data.

MODELING

Conformational energy minimization has been performed with the JUMNA program (version IV) (Lavery, 1988). This program directly employs helicoidal parameters for positioning the nucleotides in space as well as internal coordinates (dihedral and valence angles) to represent intranucleotide flexibility. It is thus particularly appropriate for studying nucleic acid structures and has already been used successfully in modeling double and triple helices (Sun et al., 1991) and processes such as hydrogen exchange (Ramstein & Lavery, 1988). Calculations were performed with the usual Flex force field (Lavery et al., 1984, 1986). Charges were calculated with a Hückel Del-Re procedure parametrized to generate monopoles which fitted potentials and fields determined by ab initio quantum

* Author to whom correspondence should be addressed.
‡ Université Paris XIII, Bobigny.
§ CNRS URA481.
∥ CNRS URA77.

0006-2960/93/0432-2098$04.00/0

chemical calculations (Lavery et al., 1984). The net charge on each phosphate group was set to −0.5e, to mimic counterion screening effects, and solvent electrostatic damping was taken into account via a sigmoidal distance-dependent dielectric function (Hingerty et al., 1985; Lavery, 1988). No cutoff distances were used.

Triple helices were built from a library of nucleotides by specifying helicoidal parameters in agreement with the Cambridge convention (Dickerson et al., 1989). Starting points used corresponded to fiber data for A and B double helices (Arnott et al., 1980) and for the Arnott triple helix (Arnott et al., 1976). The cytosines belonging to strand III of C·G×C$^+$ base triplets were protonated in order to give rise to two Hoogsteen hydrogen bonds with the guanines in strand II.

A systematic study was carried out on the stereochemically feasible sugar conformations of homopolymeric triple helices containing T·A×T or C·G×C$^+$ base triplets and of a regularly alternating sequence with both T·A×T and C·G×C$^+$ triplets. In the case of the $(C{\cdot}G{\times}C^+)_{10}$ triple helix, a study of the orientation of the third strand was also carried out. Calculations on $(T{\cdot}A{\times}T)_{10}$ and $(C{\cdot}G{\times}C^+)_{10}$ triple helices were performed using mononucleotide symmetry with respect to all helicoidal and internal parameters of each strand. For the alternating sequence, $(C{\cdot}G{\times}C^+/T{\cdot}A{\times}T)_5$, dinucleotide symmetry was imposed. These symmetry constraints allow end-effects to be avoided and simplify the conformational space to be studied by strongly reducing the number of variables to be minimized. Initial minimizations were performed by slowly releasing an increasing number of backbone, sugar, and helicoidal variables. This procedure avoided any steric constraints in the starting structures from destroying the triple helical conformation at an early stage. The minimized structures were also tested by imposing helical deformations of twist and rise to ensure that they were stable over an extended region of conformational space.

The structural properties of triple helices were analyzed using the CURVES algorithm (Lavery & Sklenar, 1989) which calculates a full set of independent helicoidal coordinates and an optimal global helical axis for nucleic acid segments with between 1 and 4 strands. Groove widths were measured at the level of the base triplets as the minimal distance between spline-fitted curves passing through the phosphorus atoms of each backbone (less 5.8 Å, representing the van der Waals radii of the phosphate groups). Groove depths were then calculated as the distance between the minimal length vector joining the backbones and the appropriate face of the base triplet (E. Stofer and R. Lavery, manuscript in preparation).

These computations were performed on a Silicon Graphics 4D/120 workstation and on a Fujitsu VP 200 computer. The JUMNA code was vectorized for the VP 200 by D. Giroud from CIRCE (Centre Inter Regional de Calcul Electronique, CNRS, Orsay, France). Molecules were visualized with the help of the INSIGHT II software commercialized by BIOSYM and fully interfaced with JUMNA program, or using the MAD interactive computer graphics program (Lahana, copyright Laboratoire Fabre, Castres, France, 1987–1989).

MATERIALS AND METHODS

$(dC)_n$ (lot CF7838101) and $(dG)_n{\cdot}(dC)_n$ (lot AA789OP12) were purchased from Pharmacia and used without purification. The samples were prepared by dissolving 1 μmol of $(dC)_n$ in 200 μL of H_2O Millipore and 1 μmol of $(dG)_n{\cdot}(dC)_n$ in 400 μL of H_2O Millipore. The concentrations were determined by UV absorbance measurements using a Beckman 3600 spectrophotometer and assuming a molar extinction coefficient ϵ_{max} around 260 nm of $(dG)_n{\cdot}(dC)_n$, 7400, and $(dC)_n$, 7400. The $(C{\cdot}G{\times}C^+)_n$ triple helix was prepared by mixing equimolecular amounts of both stock solutions at neutral pH. The pH was then adjusted to 5.7 by addition of small amounts of HCl, and samples were slowly evaporated under nitrogen to a final sample concentration around 100 mM. For Raman studies, the ionic strength of the triplex solution was varied between 100 mM and 4 M NaCl. For infrared spectroscopy, samples were studied in both H_2O and D_2O solutions at 100 mM NaCl.

Raman spectra were run using a DILOR OMARS 89 multichannel spectrophotometer coupled to an IBM AT computer. The 514-nm line of a Spectra-Physics 2025 laser was used for excitation (power at the source, 400 mW). Integration time varied between 4 and 11 s, and each spectrum is an average of 250 integrations. Infrared spectra were recorded with a Perkin-Elmer 1760 Fourier transform spectrophotometer coupled to a PE 7700 minicomputer. Usually 10 scans were accumulated. Data treatment included multiple-point base line correction and smoothing using the Savitsky and Golay algorithm.

RESULTS

We chose to study the energetic and conformational features of homopolymeric $(T{\cdot}A{\times}T)_{10}$, $(C{\cdot}G{\times}C^+)_{10}$, and alternating $(C{\cdot}G{\times}C^+/TA{\times}T)_5$ triple helices. In order to scan a large area of conformational space, we began from not only the Arnott triple helix model (Arnott et al., 1976), but also from both A and B duplex models (Arnott et al., 1980), docking the third strand using interactive molecular graphics. The impact of sugar puckering on the overall conformation was also tested by constraining the puckers in each strand to be either the C2′-endo (S-type) or the C3′-endo (N-type) families. (Following the pseudorotation notation of the sugars, O1′-endo puckers are also referred to as E-type or "eastern" conformations, and sugars falling between the categories described are denoted as SE "southeast" or NE "northeast".) As will be shown, sugar pucker turns out to be of prime importance in describing triple helical structures in the same way that it characterizes duplex DNA allomorphs.

Initial studies of the third strand orientation in the $(C{\cdot}G{\times}C^+)_{10}$ triplex showed that conformations in which the protonated homocytidine strand III was parallel to the homoguanidine strand II were much more stable. An antiparallel orientation of strand III resulted in syn nucleotides associated with S-type sugar puckers and led to strong electrostatic repulsions between the phosphodiester backbones of strands II and III. In consequence, only conformations having parallel orientations of strands II and III are discussed below.

(1) Triple Helices Derived from the Arnott A-like Model. Using the Arnott model with all C3′-endo (N-type) sugars as a starting point, the minimized triplexes with $(T{\cdot}A{\times}T)_{10}$ and $(C{\cdot}G{\times}C^+/T{\cdot}A{\times}T)_5$ sequences (R10 and R30, respectively) show that although the sugar puckering of two homopyrimidine strands (strand I and III) remains in C3′-endo family, that of homopurine strand (strand II) moves to O1′-endo family (Scheme I), which is midway between the puckers characteristic of A-DNA and B-DNA structures. Such a transition does not occur with the $(C{\cdot}G{\times}C^+)_{10}$ sequence although it can be induced for only a small energy penalty (structure R24). Scheme I shows some of the triple helix structures indirectly derived from the Arnott model and their relative conformational energies. Initially placing the sugars of a chosen strand

Scheme I: Energy-Minimized $(T\cdot A\times T)_{10}$, $(C\cdot G\times C^+)_{10}$, and $(C\cdot G\times C^+/T\cdot A\times T)_5$ Triplexes Derived from the Arnott A-like Triple Helix Model[a]

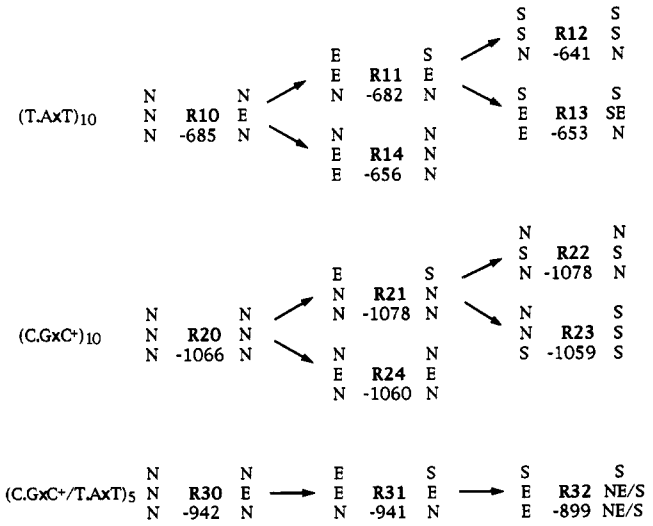

[a] Each minimization is schematized by two columns of three letters. Reading from top to bottom, the letters of each column indicate the sugar puckers in strands I, II, and III of the triple helix. The following letters are used: N, C3′-endo; NE, C4′-exo; E, O1′-endo; SE, C1′-exo; and S, C2′-endo. The left- and right-hand columns indicate the sugar conformations before and after energy minimization, respectively. The minimized conformational energies in kcal/mol and the code name of each structure are given between the two columns of letters. Arrows indicate the route followed between successive structures by constrained changes in sugar pucker.

in the O1′-endo (or E-type) pucker and then allowing them to evolve toward either S-type or N-type conformations during minimization was found to be an effective technique for locating low-energy minima. From this study it appears that the transition of the strand I sugar pucker from N-type to S-type requires little energy or is even favorable: 0.3, −1.2, and 0.1 (kcal/mol)/triplet for the triplexes $(T\cdot A\times T)_{10}$, $(C\cdot G\times C^+)_{10}$, and $(C\cdot G\times C^+/T\cdot A\times T)_5$ (R11, R21, and R31), respectively. In contrast, further modifications of the sugar puckers in strand II or any modifications of strand III are found to strongly destabilize the resulting triple helix conformations.

(*2*) *Triple Helices Derived from B-DNA and A-DNA Duplex Structures.* Extensive simulations have been carried out starting from B-like DNA structures for the Watson–Crick duplex and then, following an initial energy minimization, forming a triple helix by docking the third strand into the major groove of the duplex. All possible combinations of sugar puckering were tested. It was found that only heteronomous duplexes with an N-type sugar in strand I and an S-type sugar in strand II were capable of forming triplexes with energies comparable to those derived from the Arnott model (Scheme II, B10, B20, and B30). Note that structure B20 of the $(C\cdot G\times C^+)_{10}$ triplex is identical to the structure R22 obtained from the Arnott triple helix starting point. Scheme II also shows some of the triple helix structures which were derived from these conformations. As in the case of conformations derived from the Arnott model, it is found that the transition of sugar pucker in strand I from N-type to S-type requires a relatively little energy: 0.7, 0.1, and 0.1 (kcal/mol)/triplet for conformations B11, B21, and B31 respectively. It is worth noting that the transition of the sugar

Scheme II: Energy-Minimized $(T\cdot A\times T)_{10}$, $(C\cdot G\times C^+)_{10}$, and $(C\cdot G\times C^+/T\cdot A\times T)_5$ Triplexes Derived from B-DNA Duplex Conformations[a]

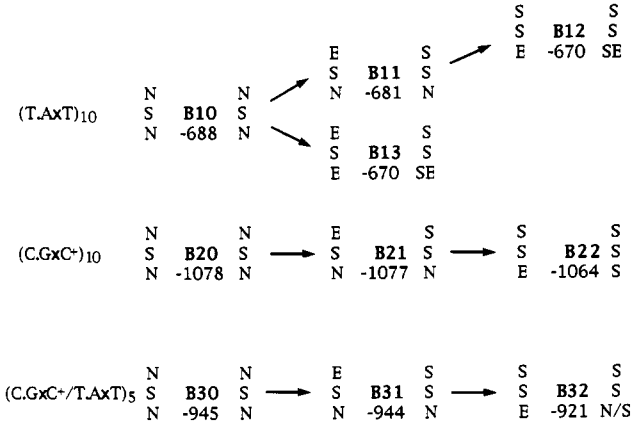

[a] Legends are as defined for Scheme I.

Table I: Helicoidal Parameters of the Minimized Triple Helices B12 $[(T\cdot A\times T)_{10}]$, B20/R22 $[(C\cdot G\times C^+)_{10}]$, and B32 $[(C\cdot G\times C^+/T\cdot A\times T)_5]$ Compared to the Arnott Triple Helix Model and Canonical A- and B-DNA Conformations

strand	Xdisp (Å)	Ydisp (Å)	rise (Å)	twist (°)	sugar pucker
		Triple Helix $(T\cdot A\times T)_{10}$			
I	−3.9	0.2	3.4	30.9	C2′-endo
II	−3.9	0.1	3.4	30.9	C2′-endo
III	−4.2	−0.3	3.4	30.9	C2′-endo
		Triple Helix $(C\cdot G\times C^+)_{10}$			
I	−3.3	−0.3	3.9	29.6	C3′-endo
II	−3.5	0.4	3.9	29.6	C2′-endo
III	−4.3	−0.3	3.9	29.6	C3′-endo
		Triple Helix $(C\cdot G\times C^+/T\cdot A\times T)_5$			
I	−3.2/−3.3	0.4/0.3	3.1/3.6	32.3/32.9	C2′-endo/C2′-endo
II	−3.4/−3.3	−0.2/−0.2	3.3/3.4	32.8/32.4	C2′-endo/C2′-endo
III	−3.8/−3.9	0.1/0.1	3.4/3.3	35.1/30.1	C3′-endo/C2′-endo
		Arnott Triple Helix Model			
I	−4.2	−0.3	3.3	30.0	C3′-endo
II	−3.6	0.6	3.3	30.0	C3′-endo
III	−4.4	0.1	3.3	30.0	C3′-endo
		A-DNA Double Helix (Arnott-80)			
	−5.28	0.0	2.56	32.7	C3′-endo
		B-DNA Double Helix (Arnott-80)			
	0.0	0.0	3.38	36.0	C2′-endo

pucker in strand III from N-type to S-type again needs more energy, but is nevertheless easier than in the case of the Arnott-derived conformations: 1.1, 1.3, and 2.3 (kcal/mol)/triplet for conformations B12, B22, and B32, respectively.

The same simulation procedure has been used to scan possible triple helix structures derived from A-like DNA structures (which have a much stronger inclination and a smaller rise than the Arnott triple helix model). It was found that the only energetically feasible triplexes which could be built in this way are those with N-type sugars in strands I and III and S-type sugars in strand II. These structures converged to the same energy minimum as the triplexes derived initially from B-DNA conformations.

Tables I–III summarize the main conformational features of the triple helices discussed above in comparison with those of the Arnott triple helix model and canonical double-stranded A- or B-DNA.

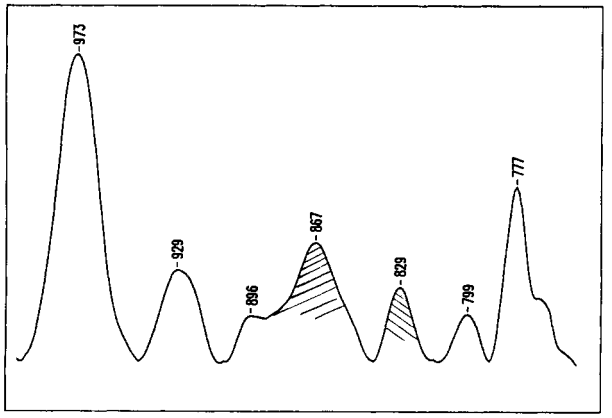

FIGURE 1: FTIR spectra of the $(C\cdot G\times C^+)_n$ triple helix in the spectral region 1000–750 cm^{-1} recorded in D_2O. S-type sugar: \\\. N-type sugar: ///.

Table II: Backbone Dihedrals of the Minimized Triple Helices B12 $[(T\cdot A\times T)_{10}]$, B20/R22 $[(C\cdot G\times C^+)_{10}]$, and B32 $[(C\cdot G\times C^+/T\cdot A\times T)_5]$ Compared to the Arnott Triple Helix Model and Canonical A- and B-DNA Conformations

strand	χ	α	β	γ	δ	ϵ
			Triple Helix $(T\cdot A\times T)_{10}$			
I	59	−67	−178	55	134	−172
II	58	−62	−179	51	132	−173
III	56	−67	−179	55	129	−172
			Triple Helix $(C\cdot G\times C^+)_{10}$			
I	19	−72	177	66	80	−161
II	58	−62	−173	51	140	−174
III	6	−76	−179	67	79	−157
			Triple Helix $(C\cdot G\times C^+/T\cdot A\times T)_5$			
I	62/70	−70/71	178/−179	57/56	138/139	−172/−173
II	73/67	−59/−69	179/−179	50/51	137/136	−178/−170
III	15/61	−69/136	−175/−168	178/67	83/142	−159/−173
			Arnott Triple Helix Model			
I	28	−46	174	39	81	−156
II	33	−66	180	55	81	−161
III	27	−53	172	47	81	−160
			A-DNA Double Helix (Arnott-80)			
	21	−75	181	59	78	−155
			B-DNA (Arnott-80)			
	78	−41	136	37	139	−133

Table III: Groove Geometry of the Minimized Triple Helices B12 $[(T\cdot A\times T)_{10}]$, B20/R22 $[(C\cdot G\times C^+)_{10}]$, and B32 $[(C\cdot G\times C^+/T\cdot A\times T)_5]$ Compared to the Arnott Triple Helix Model and Canonical A- and B-DNA Conformations

	groove width (Å)		groove depth (Å)	
DNA structures	minor	major	minor	major
triple helix $(T\cdot A\times T)_{10}$	5.9	10.0	3.7	10.9
triple helix $(C\cdot G\times C^+)_{10}$	7.9	8.8	2.8	8.0
triple helix $(C\cdot G\times C^+/T\cdot A\times T)_5$	5.3	7.2	4.0	10.1
Arnott triple helix model	10.5	3.3	1.3	9.9
A-DNA double helix	10.8	3.0	0.5	11.2
B-DNA double helix	5.6	11.2	5.1	6.1

(3) Vibrational Spectroscopy of the $(C\cdot G\times C^+)_n$ Triple Helix. (a) FTIR Spectroscopy. Figure 1 shows the FTIR spectrum of $(C\cdot G\times C^+)_n$ between 1000 and 750 cm^{-1} recorded in D_2O solution. This spectral region contains absorption bands arising from vibrational modes of the deoxyribose residues coupled to phosphodiester chain vibrations. Some of these modes are very sensitive to the sugar backbone conformation and are efficient markers of the DNA secondary structure (Taillandier et al., 1985). The triple helix spectra have been interpreted by comparison with the spectra of

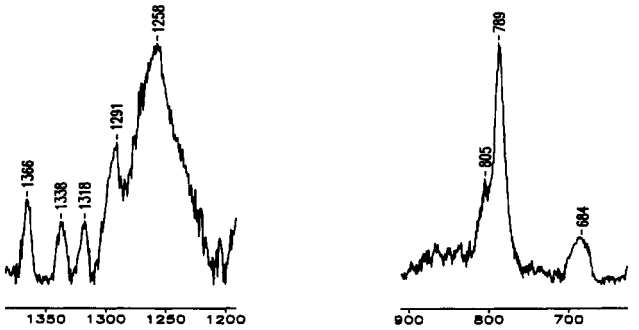

FIGURE 2: Raman spectrum of $(C\cdot G\times C^+)_n$ triple helix in the spectral regions (a, right) 900–600 cm^{-1} and (b, left) 1400–1200 cm^{-1}.

double-stranded $(dG)_n\cdot(dC)_n$. In the triplex spectrum, two sugar absorptions are detected at 867 and 829 cm^{-1}. The former, which is always present in A-form nucleic acid spectra, is a characteristic IR marker of the N-type sugar conformation. The latter mode is observed in B-form DNA spectra and shows the existence of S-type sugars. In the $(C\cdot G\times C^+)_n$ spectrum, the relative intensity of the absorption band located at 867 cm^{-1} is about twice that of the 829-cm^{-1} absorption band. This result indicates a sugar conformation ratio of two N-type sugars for one S-type within this triple helix.

(b) Raman Spectroscopy. The 900–615-cm^{-1} Raman spectral region contains a vibration mode of the dG residue which is assigned to a coupling between a guanine ring breathing mode and a vibration of the deoxyribose. This model is very sensitive to the conformation of the sugar pucker and to the glycosidic torsion angle of the dG residue. Several previous Raman studies and normal-mode coordinate analysis of double-stranded DNA (Thamann et al., 1981; Nishimura et al., 1986; Letellier et al., 1986; Peticolas et al., 1987) have shown that this mode appears around 685 cm^{-1} in B-form DNA (dG: C2′-endo/anti) and is shifted to 660 cm^{-1} in A-form DNA (dG: C3′-endo/anti) and to 625 cm^{-1} in Z-form DNA (dG: C3′-endo/syn). In the present work, a strong peak is observed at 684 cm^{-1} (Figure 2a), showing that the dG residues in the $(C\cdot G\times C^+)_n$ triple helix have an S-type sugar conformation associated with a glycosidic torsion in the anti conformation. No peak is detected around 660 cm^{-1}, confirming the absence of anti-dG residues with sugars having an N-type geometry. However, the sugars of the three strands in the triplex cannot be in the S-type conformation. A Raman line is clearly observed at 805 cm^{-1} (Figure 2a). This line is assigned to a marker band of A-form nucleic acids. It is strongly related to the torsional angle δ reflecting the N-type sugar pucker. The existence of both S-type and N-type sugars in $(C\cdot G\times C^+)_n$ triplex is confirmed by the analysis of the 1400–1200-cm^{-1} spectral region (Figure 2b). This region is well-known to contain peaks characteristic of the deoxycytidine and deoxyguanosine conformations. The triplet at 1366–1338–1318 cm^{-1} reflects the C2′-endo/anti deoxyguanosine conformation; the very strong peak at 1258 cm^{-1} is assigned to the C3′-endo/anti deoxycytidine. The 1291-cm^{-1} peak is due to cytosine base vibrations whatever the DNA conformation (A or B) (Nishimura et al., 1986). One may note that the relative intensities of the deoxycytidine and deoxyguanosine markers can be explained by the stoichiometry of the triplex: two cytosine bases for one guanine. The Raman data thus show that, in the $(C\cdot G\times C^+)_n$ triple helix, the purine strand sugars adopt an S-type geometry while pyrimidine strand sugars are in an N-type geometry.

FTIR studies performed on the $(T\cdot A\times T)_n$ triple helix structures have shown that a conformational transition could

be induced by decreasing the hydration of the $(T{\cdot}A{\times}T)_n$ films (Liquier et al., 1991). In order to examine the conformational flexibility of $(C{\cdot}G{\times}C^+)_n$ triple helix, we have recorded the Raman spectra at various ionic strengths ([NaCl] = 0.1 M → 4.0 M). This choice was made taking into account the fact that the $(dG)_n{\cdot}(dC)_n$ duplex exhibits a B → A conformational transition upon increasing ionic strength between the same limits (Nishimura et al., 1986). However, in the case of the $(C{\cdot}G{\times}C^+)_n$ triple helix, no Raman spectral variations were observed as a function of the [NaCl] concentration and thus no evidence of a conformational transition exists.

DISCUSSION

In the light of the present study, using energy minimization coupled with constrained changes in sugar puckering, it emerges that DNA triple helices can form a family of more or less B-like conformations which are both energetically and stereochemically feasible. In many cases, sugar puckers can be changed with relatively small energy costs. Before discussing these findings in detail, it should be stressed once again the energies of all the conformations presented are rather similar and their absolute ordering should not be considered as significant due to the approximate nature of the force field employed, notably as concerns the very simple modeling of solvation effects.

(1) $(T{\cdot}A{\times}T)_{10}$ Triplex. The calculations demonstrate the conformational flexibility of $(T{\cdot}A{\times}T)_{10}$ triple helix with respect to sugar puckering (Schemes I and II) and the possibility of conformations containing mainly S-type sugars. These results can be correlated with data from Fourier transform infrared spectroscopy (Liquier et al., 1991). The usual sugar conformation IR marker bands reflect mainly S-type sugars in solution. However, if the relative humidity (RH) of a $(T{\cdot}A{\times}T)_n$ film is reduced from 100% to 47%, modifications occur in the infrared spectrum with the emergence of an N-type sugar IR marker. This could be assigned to a partial transition of the sugar pucker ring conformation versus the relative humidity variation. The present energy calculations show that the S-type sugar $(T{\cdot}A{\times}T)_{10}$ triple helix B12 agrees well the FTIR spectrum of $(T{\cdot}A{\times}T)_n$ obtained in films at 100% RH. The conformational transition which is apparently detected by infrared spectroscopy in films at low RH could also be explained by a transition from structure B12 to B11 (Scheme II) in which the third strand has N-type sugars. The structures derived from B-DNA (Arnott et al., 1980) coordinates are therefore in better agreement with FTIR data than those coming from the Arnott model.

Structural analysis of the $(T{\cdot}A{\times}T)_{10}$ triplex conformation B12 (Tables I–III) shows Xdisp, Ydisp, rise, and twist values similar to the Arnott triple helix structure; howevr, the glycosidic angles are considerably closer to those of B-DNA duplexes, and this is reflected in the groove geometry of the strand I–II duplex which is much closer to B-DNA and than to the Arnott triple helix conformation.

(2) $(C{\cdot}G{\times}C^+/T{\cdot}A{\times}T)_5$ Triplex. The present calculations show that the alternating triplex $(C{\cdot}G{\times}C^+/T{\cdot}A{\times}T)_5$ can also adopt sugar conformations which are very different from those of the Arnott triple helix model. The $(C{\cdot}G{\times}C^+/T{\cdot}A{\times}T)_5$ conformations derived from the B-DNA starting geometry can easily adopt predominantly S-type sugars (conformation B32 in Scheme II and Table II). Only the cytidines of strand III resist this passage. This finding is in accord with recent NMR studies performed on a 31-base DNA oligonucleotide which folds to form an intramolecular triplex (Macaya et al., 1992) containing an alternating $(C{\cdot}G{\times}C^+/T{\cdot}A{\times}T)$ sequence. This study shows that both the purines and the thymidines of the triplex have predominantly S-type sugars and only cytidines in the third strand can have a large proportion of N-type sugars.

The conformational characteristics of the B32 triplex (Tables I and III) show slightly decreased Xdisp and increased twist compared to the Arnott model, bringing the structure closer to the B-form. This is also the case for the glycosidic angles (with a single exception for the cytidines in strand I) and for the minor groove geometry.

(3) $(C{\cdot}G{\times}C^+)_{10}$ Triple Helix. We recall that preliminary calculations on the $(C{\cdot}G{\times}C^+)_{10}$ triple helix enabled us to eliminate an antiparallel orientation of strand III with respect to strand II for energetical reasons. Of the parallel strand conformations obtained, the conformations R21 and R22 have S-type and N-type sugars in agreement with the ratio 1:2 deduced from the relative intensities of the FTIR bands at 867 and 829 cm^{-1}. However, only one of these conformations, R22, is also in agreement with the Raman data showing the C2′-endo/anti conformation found to be associated with the guanosine strand. It thus seems possible to conclude that R22 best represents the solution conformation of $(C{\cdot}G{\times}C^+)_n$ triple helices.

It is also worth noting that no significant Raman peak at 830 cm^{-1}, known to be characteristic of S-type sugars, is detected for this triplex, although all other markers of deoxyguanosine with an S-type sugar conformation are present. The lack of significative intensity at 830 cm^{-1} is classically observed in the case of the coexistence of the A and B conformations (Nishimura et al., 1986). This is agreement with the conformational characteristics of the $(C{\cdot}G{\times}C^+)_{10}$ R22/B20 triplex (Tables I–III) which again lies between the A-like Arnott model and B-like parameters in terms of helicoidal parameters and groove geometry. It can be noted however that only the guanosine strand has B-like glycosidic angles and that the rise is larger than that of canonical B-DNA due to electrostatic repulsion between successive positively charged $C{\cdot}G{\times}C^+$ base triplets.

In conclusion, we have shown, by the use of JUMNA molecular mechanics calculations combined with vibrational spectroscopy, that triple helix structures containing S-type sugars are stereochemically and energetically feasible and are in accord with the present spectroscopic data and recent NMR studies. Such conformations are thus unlike the triple helix conformation proposed by Arnott and co-workers on the basis of fiber diffraction. It also appears probable that, for at least certain base sequences, sugar conformations (especially in strands I and II) may be changed rather easily.

ACKNOWLEDGMENT

We wish to thank the CIRCE (Centre Inter-Regional de Calcul Electronique–CNRS–Orsay) for computational facilities and particularly D. Giroud and J. M. Teuler for their help in adapting the JUMNA code.

REFERENCES

Arnott, S. & Bond, P. J. (1973) *Nature 244*, 99–101.
Arnott, S., & Selsing, E. J. (1974) *J. Mol. Biol. 88*, 509–521.
Arnott, S., Bond, P. J., Selsing, E., & Smith, P. J. C. (1976) *Nucleic Acids Res. 3*, 2459–2470.
Arnott, S., Chandrasekharan, R., Birdsall, R. D. L., Leslie, A. G. W., & Ratliff, R. L. (1980) *Nature 283*, 743–745.
Dickerson, R. E., Bansal, M., Calladine, C. R., Diekmann, S., Hunter, W. N., Kennard, O., Lavery, R., Nelson, H. C. M.,

Olson, W. K., Saenger, W., Shakked, Z., Sklenar, H., Soumpasis, D. M., Tung, C. S., Von Kitzing, E., Wang, A. H. J., & Zhirkin, V. B. (1989) *J. Biomol. Struct. Dyn. 6*, 627–634.

Francois, J. C., Saison-Bemhoaras, T., Thuong, N. T., & Hélène, C. (1989) *Biochemistry 28*, 9617–9619.

Hélène, C., Thuong, N. T., Saison Behmoaras, T., & Francois, J. C. (1989) *Trends Biotechnol. 7*, 310–315.

Hingerty, B., Richie, R. H., Ferrel, T. L., & Turner, J. E. (1985) *Biopolymers 24*, 427–439.

Lavery, R. (1988) in *Structure and Expression, Volume 3, DNA bending and curvature* (Olson, W. K., Sarma, M. H., Sarma, R. H., & Sundaralingam, M., Eds.) pp 191–211, Adenine Press, Guilderland, NY.

Lavery, R., & Sklenar, H. (1989) *J. Biomol. Struct. Dyn. 4*, 655–667.

Lavery, R., Zakrzewska, K., & Pullman, B. (1984) *J. Comput. Chem. 5*, 363–373.

Lavery, R., Parker, I., & Kendrick, J. (1986) *J. Biomol. Struct. Dyn. 4*, 443–461.

Le Doan, T., Perrouault, L., Praseuth, D., Habhoub, N., Decout, J. L., Thuong, N. T., Lhomme, J., & Hélène, C. (1987) *Nucleic Acids Res. 15*, 7749–7760.

Letellier, R., Ghomi, M., & Taillandier, E. (1986) *J. Biomol. Struct. Dyn. 3*, 671–687.

Liquier, J., Coffinier, P., Firon, M., & Taillandier, E. (1991) *J. Biomol. Struct. Dyn. 9*, 437–445.

Lyamichev, V. L., Mirkin, S. M., Frank-Kamenetskii, M. D., & Cantor, C. R. (1988) *Nucleic Acids Res. 16*, 2165–2178.

Macaya, R. F., Schultze, P., & Feigon, J. (1992) *J. Am. Chem. Soc. 114*, 781–783.

Maher, L. J., III, Wold, B., & Dervan, P. B. (1989) *Science 245*, 725–730.

Mirkin, S. M., Lyamichev, V. I., Drusklyak, K. N., Dobrynin, V. N., Filippov, S. A., & Frank-Kamenetskii, M. D. (1987) *Nature 330*, 495–497.

Moser, H. E., & Dervan, P. B. (1987) *Science 238*, 645–650.

Nishimura, Y., Torigoe, C., & Tsuboĭ, M. (1986) *Nucleic Acids Res. 14*, 2737–2748.

Peticolas, W. L., Kubasek, W. L., Thomas, G. A., & Tsuboĭ, M. (1987) in *Biological Applications of Raman Spectroscopy* (Spiro, T. G., Ed.) Vol. 1, pp 81–133, Wiley, New York.

Rajagopal, P., & Feigon, J. (1989) *Biochemistry 28*, 7859–7870.

Ramstein, R., & Lavery, R. (1988) *Proc. Natl. Acad. Sci. U.S.A. 85*, 7231–7235.

Santos, C. D. L., Rosen, M., & Patel, D. (1989) *Biochemistry 28*, 7282–7289.

Strobel, S. A., & Dervan, P. B. (1990) *Science 249*, 72–75.

Sun, J. S., Mergny, J. L., Lavery, R., Montenay-Garestier, T., & Hélène, C. (1991) *J. Biomol. Struct. Dyn. 9*, 411–425.

Taillandier, E., Liquier, J., & Taboury, J. A. (1985) in *Advances in Infrared and Raman Spectroscopy* (Clark, R. H. J., & Hester, R. E., Eds.) Vol. 12, pp 65–114, Academic Press, Wiley-Heyden, New York.

Thamann, T. J., Lord, R. C., Wang, A. H. J., & Rich, A. (1981) *Nucleic Acids Res. 9*, 5443–5457.

Thomas, G. A., & Peticolas, W. L. (1983) *J. Am. Chem. Soc. 105*, 993–996.

Wells, R. D., Collier, D. A., Hanvey, J. C., Shimizu, M., & Wohlrab, F. (1988) *FASEB J. 2*, 2939–2949.